The influence of uplift water pressures on the deformations and stability of flood embankments

L'influence des sous-pressions sur la déformation et la stabilité des digues

C.M.H.BAUDUIN, Belgium
C.J.B.MOES, Delft Geotechnics, Netherlands
M.VAN BAALEN, Delft Geotechnics, Netherlands

SYNOPSIS: In the Netherlands, flood embankments are extensively used along the North Sea coast and the rivers of the Meuse-Rhine delta. The soil in the western part of the Netherlands mostly consists of Holocene clay and peat layers, overlying a Pleistocene sand stratum which is more or less in open contact with the river or the sea. Under certain circumstances, the water pressures in the pervious sand stratum may cause uplifting of the overlying semi-impervious layers, which may be determinating for the embankment's behaviour during storm surge or high river discharge. A method is presented to predict whether uplift is likely to occur under design flood conditions and to assess the length and location of the uplift area and to analyse the stability and deformation of the embankment.

1. INTRODUCTION

Under the said circumstances, time dependent variations of the water level in the river provoke time and distance dependent variations of the pore water pressure in the pervious sand stratum. The water pressure in the sand stratum during storm or high river discharge can increase until it reaches the pressure exerted by the weight of the overlying semi-impervious layers.

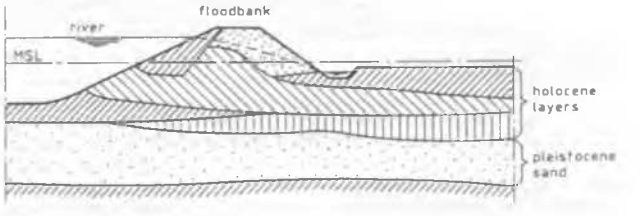

fig. 1. embankment on typical Dutch soil strata

From that moment, the effective contact stress between the soft Holocene foundation layer and the stiff sand stratum is lost. This phenomenon is called 'uplift'. When the overlying layers are very lightweighted (e.g. peat or very organic clay), this loss of shear stress may lead to heavy compression of the holocene layers beyond the toe of the inner slope of the embankment and subsequently to loss of function of the embankment.

Faced with the task to supply rules for the design of embankments along the river Thames under uplift conditions, the British Building Research Establishment made safe, conservative assumptions (Padfield et al, 1983). It was assumed that, in extreme cases, the resistance exerted by the marsh to the toe of the embankment could drop as low as that, corresponding to a hydrostatic waterpressure. Facing the same question for the embankments along the rivers of the upper Meuse-Rhine delta, the Dutch Technical Advisory Committee for Embankments advised to take only the drained cohesion of the layers beyond the toe into account in the stability analyses under uplift conditions.

Both methods mentioned are somewhat rough approximation for the interaction problem, as they do not take the real behaviour of the embankment (in particular its deformations) into account. The following factors are considered to affect the magnitude of the displacement at the toe of the embankment and hence the magnitude of crest settlements under uplift conditions.

- The location and length of the uplift area
- The mobilized shear strength in the active area before uplift.
- The loss of shear resistance along the interface surface during uplift conditions.
- The stiffness of the marsh.

2 CALCULATION OF THE PORE WATERPRESSURE AND THE LOCATION AND LENGTH OF THE UPLIFT AREA

2.1 Pore waterpressure as long as no uplift occurs

For the geo-hydrological conditions prevailing in the Meuse-Rhine delta (see fig. 2) it has been shown that the time and distance dependent response of the waterpressure in the pervious sand due to the variations of the waterlevel in the river (tidal, storm surge and/or high river discharge) is mainly governed by the consolidation process in the bottom layer and the aquitard (Barends, 1982; Bauduin and Barends, 1988). The

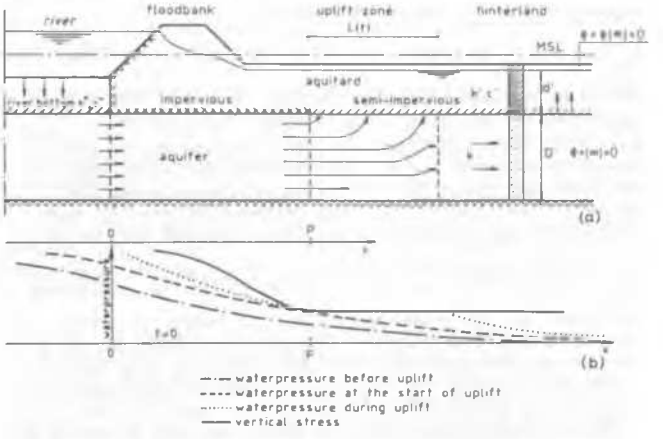

fig. 2. Geohydrological schematisation and pore water pressures during uplift.

analytical solutions for this model are presented in table I. These solutions can be used in Marsland's methodology to assess the basic geo-hydrological parameters using the measured response under normal circumstances and to predict the waterpressure under design flood conditions (see fig. 3)

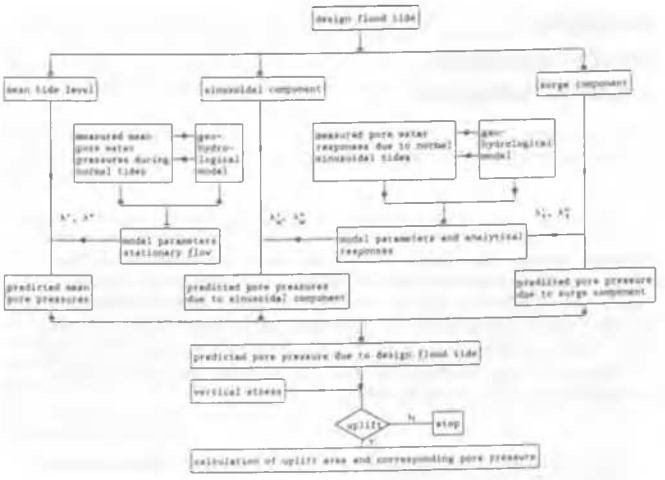

fig. 3. Flowchart for calculation of pore presures during design flood and verification for uplift

The leakage factors for stationary flow λ' and λ'' and for tidal variations λ'_ω and λ''_ω can be assessed using the response of at least two piezometers (but preferably more since this increases the reliability of the answer). The two-step-method is illustrated for tidal variations :

- determination of λ'_ω based on the measured damping of the response of the piezometers located at x>P to one-another:

$$\lambda'_\omega = x_{ij}/\ln(\phi_i/\phi_j) \qquad \text{(eq. 1)}$$

  In which: x_{ij} is the distance between the piëzometers and ϕ_i, ϕ_j the measured piëzometric levels.

- Determination of λ''_ω by solving the equations for tidal variation in table 1 in which one puts the value of λ'_ω as assessed in the first step (eq. 1).

The tidal leakage factors for other frequencies of the sinusoidal variation of the water level, can be derived from the measured ones, as for a given geohydrological situation the following is valid:

$$\lambda'_\omega \sqrt{\ } \omega = \Omega = \text{constant} \qquad \lambda''_\omega \sqrt{\ } \omega = \Omega = \text{constant} \qquad \text{(eq. 2)}$$

The time dependent leakage factors λ'_t and λ''_t for a step variation of the water level, cannot be measured directly. When the time t in the formulas for λ'_t and λ''_t is short compared to the hydrodynamic period of the aquitard and the river bottom layer (being equal to 2d'*d'/c' and 2d"*d"/c"), the leakage factors for step variations are related to the tidal leakage factors by:

$$\lambda'_t = \frac{1}{1{,}287}\sqrt{(4\omega t)}.\lambda'_\omega \qquad \lambda''_t = \frac{1}{1{,}287}\sqrt{(4\omega t)}.\lambda''_\omega \qquad \text{(eq. 3)}$$

In order to verify whether uplift is likely to occur during design water level, the potential heads given by the equations in table I must be converted into water-pressures. Taking the reference potential head equal to zero on the phreatic line, as done in table I, the potential heads given in this table can then directly be converted into pressures by multiplying by the unit weight of the pore water.

Tabel I

Waterpressure variation in aquifer as a function of time and distance.

waterlevel variation	Response in aquifer as a function of time and place
Stationary	$0<X<P \rightarrow \phi(X) = [\phi_s-\phi_p]\cdot[1-\frac{X}{P}]+\phi_p$ $X>P \rightarrow \phi(X') = \phi_p\cdot\exp(-X'/\lambda')$ with $X' = X-P$ in which : $\phi_s = \frac{H}{1+\frac{\lambda''}{\lambda'}\frac{P}{\lambda''}\coth(B/\lambda'')}$ $\phi_p = \frac{H}{1+\frac{\lambda''}{\lambda'}\frac{P}{\lambda''}\coth(B/\lambda'')}$ $\lambda' = \sqrt{(\frac{k\cdot d'\cdot D}{k'})}$ $\lambda'' = \sqrt{(\frac{k\cdot d''\cdot D}{k''})}$
Tidal $\omega = 2\pi/T$	$0<X<P \rightarrow \phi(X,t) = [\phi_s-\phi_p]\cdot[1-\frac{X}{P}]+\phi_p$ $X>P \rightarrow \phi(X;t) = \frac{\cos(\omega t-X'\cdot\tan(\frac{\pi}{8})/\lambda'_\omega-\beta)\cdot\exp(-X'/\lambda'_\omega)}{[(1+h_1)^2+h_2^2]^{1/2}}\cdot\phi_p$ in which $\phi_s = \frac{H_s\cdot\cos(\omega t-\gamma)}{[(1+m_1)^2+m_2^2]^{1/2}}$ $\phi_p = \frac{H_s\cdot\cos(\omega t-\beta)}{[(1+m_1)^2+m_2^2]^{1/2}}$ $m_1 = \frac{[1+P/\lambda'_\omega]\cdot\sinh(2\cdot B/\lambda''_\omega)-\sin(2\cdot B\cdot\tan(\pi/8)/\lambda''_\omega)\cdot\tan(\pi/8)\cdot P/\lambda'_\omega}{(\cosh(2B/\lambda''_\omega)-\cos(2\cdot B\cdot\tan(\pi/8)/\lambda''_\omega))\cdot([1+P/\lambda'_\omega]^2+(P\cdot\tan(\pi/8)/\lambda'_\omega)^2)}$ $m_2 = \frac{(1+P/\lambda'_\omega)\cdot[\sin(2B\cdot\tan(\pi/8)/\lambda''_\omega)]+\sinh(2\cdot B/\lambda''_\omega)\cdot P\cdot\tan(\pi/8)/\lambda'_\omega}{(\cosh(2\cdot B/\lambda''_\omega)-\cos(2\cdot B\cdot\tan(\frac{\pi}{8})/\lambda''_\omega))\cdot([1+P/\lambda'_\omega]^2+(P\cdot\tan(\pi/8)/\lambda'_\omega)^2)}$ $h_1 = \sqrt{(\frac{\lambda''_\omega}{\lambda'_\omega})}\cdot\frac{(1+P/\lambda''_\omega)\cdot\sinh(2\cdot B/\lambda''_\omega)+\sin(2\cdot B\cdot\tan(\pi/8)/\lambda''_\omega)\cdot P\cdot\tan(\pi/8)/\lambda''_\omega}{(\cosh(2\cdot B/\lambda''_\omega)-\cos(2\cdot B\cdot\tan(\frac{\pi}{8})/\lambda''_\omega))}$ $h_2 = \sqrt{(\frac{\lambda''_\omega}{\lambda'_\omega})}\cdot\frac{(P\cdot\tan(\pi/8)/\lambda''_\omega)\cdot\sinh(2\cdot B/\lambda''_\omega)-(1+P/\lambda''_\omega)\cdot\sin(2\cdot B\cdot\tan(\pi/8)/\lambda''_\omega}{(\cosh(2\cdot B/\lambda''_\omega)-\cos(2\cdot B\cdot\tan(\frac{\pi}{8})/\lambda''_\omega))}$ $\lambda'_\omega = \frac{1}{\cos(\pi/8)}\sqrt{(\frac{k\cdot D}{k'})}\cdot\sqrt{(c'/\omega)}$ $\lambda''_\omega = \frac{1}{\cos(\pi/8)}\sqrt{(\frac{k\cdot D}{k''})}\cdot\sqrt{(c''/\omega)}$ $\beta = \operatorname{atan}(\frac{h_2}{1+h_1})$ $\gamma = \operatorname{atan}(\frac{m_2}{1+m_1})$
Sudden surge	$0<X<P \rightarrow \phi(X,t) = [\phi_s(t)-\phi_p(t)]\cdot[1-\frac{X}{P}]+\phi_p$ $X>P \rightarrow \phi(X;t) = \phi_p(t)\cdot\exp(-X'/\lambda'_t)$ with $X' = X-P$ in which: $\phi_p = \frac{H}{1+\frac{P+\lambda''}{\lambda'_t}\frac{c}{\lambda''_t}\coth(B/\lambda''_t)}$ $\phi_s = \frac{H}{1+\frac{\lambda''}{\lambda'_t}\frac{c}{\lambda''_t}\coth(B/\lambda''_t)}$ $\lambda'_t = [(\frac{k'}{k\cdot D}\cdot\sqrt{(\frac{1}{2\cdot c'}\cdot s_t)}\cdot\coth(\frac{d'}{\sqrt{(2\cdot c'\cdot s_t)}})]^{-1/2}$ $\lambda''_t = [(\frac{k''}{k\cdot D}\cdot\sqrt{(\frac{1}{2\cdot c''}\cdot s_t)}\cdot\coth(\frac{d''}{\sqrt{(2\cdot c''\cdot s_t)}})]^{-1/2}$
Special cases	1. No bottomlayer : $\lambda'' = 0$, $\lambda''_\omega = 0$ and $\lambda''_t = 0$ 2. Homogeneous aquitard: $P = 0$ 3. Very wide river, sea: $B = \text{infinite}$

2.2 Pore Water Pressure during Uplift.

When the waterpressure somewhere in the sand layer tends to become greater than the local total vertical stress, no further increase of the waterpressure is possible. The formulas given in table I are no longer valid because waterpressure redistribution will occur. An approximated solution can be found in the case of stationary flow for the geo-hydrological conditions of fig. 2. The length L of the uplifted area is found by solving the following implicit equation:

$$L = \frac{2D}{\pi}\,\mathrm{acosh}\left[\frac{1}{\sin\left[\frac{D\phi_g}{\lambda'(H-\phi_g)}\left[\frac{\pi\lambda''}{2D}+\mathrm{arcsinh}\left(\frac{\sinh((P+L)\pi/2D)}{\cosh(L\pi/2D)}\right)\right]\right]}\right] \qquad \text{(eq. 4)}$$

in which: L = length of the uplifted area
D = thickness of the aquifer
P = distance between the river and the beginning of the uplift area.
ϕ_g = potential head in uplift zone ($\phi_g = \sigma_v/\gamma_w$)

The corresponding distribution of the water pressures during uplift is approximately given by:

$$x = 0 \rightarrow \phi(0) = \frac{H\ 2D\ \mathrm{arcsinh}\ \alpha + \lambda'\ \pi\ \phi_g}{2D\ \mathrm{arcsinh}\ \alpha + \lambda'\ \pi} \qquad \text{(eq. 5)}$$

$$0 < x < P \rightarrow \phi(x) = (\phi(0) - \phi_g)\left(1 - \frac{x}{P}\right) + \phi_g$$

$$P < x < P + L \rightarrow \phi(x) = \phi(g)$$

$$x > P + L \rightarrow \phi(x) = \phi_g \exp(x'/\lambda') \;\&\; x = x' + P + L$$

In which: $\alpha = \dfrac{\sinh((P + L)\ \pi/2D)}{\cosh(L\pi/2D)}$

The basic assumption underlying the above mentioned formulas is that the flow at the end of the uplift area is purely horizontal, which is of course not true. This assumption leads to an overestimation of L. A first correction can be made by replacing P in eq. 4 by $P+(2D\ln 2)/\pi$. A correcter method has been proposed by Barends (1988).
Exact solutions for the time dependent development of the uplift area are hard to find because of the non-linearity introduced at the interface of the layers during the uplift. An approximate solution can be found however by replacing λ' and λ'' by λ'_t and λ''_t in the eq. 4 and 5. It can be shown that this solution is "exact" at the start of the uplift and that it tends towards the solution for stationary flow for large values of t.

3 DEFORMATIONS AND STABILITY UNDER UPLIFT CONDITIONS.

3.1 The basic mechanism's

The significance of uplift on the deformation and stability of flood embankments has been first reported by Marsland (1961), analyzing the failure of the eastern bank of the river Darent (Thames Valley). In order to investigate the behaviour during uplift, Padfield et al (1983) performed series of centrifuge tests, which delivered the key to the understanding of the basic mechanism. Several attempts have been made to simulate embankment behaviour under uplift conditions using elasto-plastic FEM analysis (Vermeer et al, 1984; Bauduin, 1985; Teunissen et al, 1986). These exercises have shown that FEM analysis is probably the most suitable approach to model the embankment behaviour during uplift conditions.
Figure 4. shows the results of FEM analysis for the Wolpherense dike in the Netherlands (Vermeer et al, 1984). Indicated are the conventional failure mechanism (Bishop) and the uplift failure mechanism, ofwhich the latter proved to be the most critical.

Fig. 4a. Plastic zone during failure of the Wolpherense Dike due to uplift.

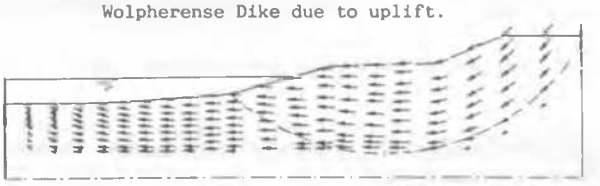

Fig. 4b. Corresponding velocity field and indication of most critical slip circle

The results of the above mentioned centrifuge tests and finite element calculations properties suggest the following behaviour for embankments, built on normally consolidated foundation layers with low stiffness parameters compared to those of the embankment's material.

In normal circumstances (i.e. no uplift occurs), the circular slip surface in fig. 5a is more critical than the elongated surface in fig. 5b. The part ABC of the potential sliding mass is balanced by shear stresses along AB and by the force I.

The shear resistance along the interface between the Holocene layers and the Pleistocene sand stratum restricts the horizontal displacements of the soft Holocene foundation layers by "pinning" it onto the stiff sand stratum. Under uplift conditions however, the shear resistance at the interface between the soft Holocene layers and the sand stratum drops to zero. As a result, large horizontal strain leads to displacement of the toe of the embankment, because a new force equilibrium has to develop under this new interface condition: The force I is to be balanced by neutral to passive forces in the area B'D' (5b) well beyond area BD (5a). The uplifted mash works as a compressed beam transferring the force I from the active area to the resistant area beyond the uplift zone.

Embankment failure during uplift can be caused by one of the following conditions:

- The passive area B'D' or the uplifted part of the marsh cannot supply the passive resistance to balance I.
- The elastic and/or plastic deformations of the passive area and the compressed part of the marsh are unacceptable.

In this last case, the failure surface never needs to re-emerge: the embankment mobilizes the full shear resistance in the active area and shows unacceptable displacement at the crest.

A factor of safety against failure can be assessed in both uplift and non-uplift conditions using stability analysis. However this factor of safety alone is not sufficient to judge whether the embankment is capable to fulfill its function under design conditions, since displacements are not taken into account.

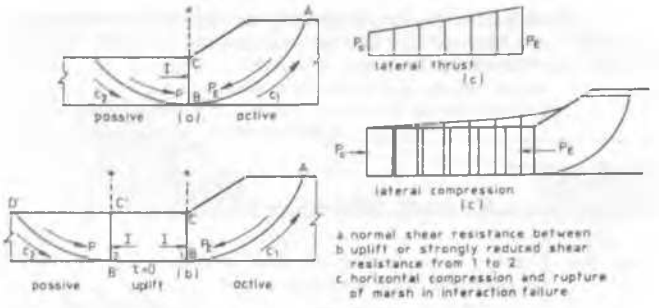

Figure 5. Failure mechanisms with and without uplift

3.2 The simplified model, an Adapted Slip Surface Method (ASSM).

The above studies have emerged in a simple, Bishop/ Spencer oriënted Adapted Slip Surface Method (ASSM), which provides an inexpensive and less time consuming alternative for FEM analysis. It must be emphasized that its verification is still limited. However, up to now the method seems to reproduce answers, comparable with those of FEM analysis (van Baalen, 1988).

3.2.1 Stability analysis under uplift conditions

The principal adaptions are that two underlying assumptions of the conventional slip surface analysis are abandoned: the shape of the slip surface as well as the degree of mobilization of available shear strength in the active and the passive area are no longer directly related.
In conventional slip surface analysis this degree of mobilization is assumed to be constant along the slip surface. In general however, the active area has a relatively high degree of mobilization under all circumstances: the passive area generally fails last. In consequence, with slip surface analysis and relatively high overall stability factors, the inter slice forces are not calculated properly: they are overestimated because the mobilized shear strength in the active area is underestimated. In ASSM a first adaption is made by assuming a relatively high degree of mobilization in the active area.
Several potential slip surfaces are analysed to find the minimum safety factor. The factor of safety in ASSM is defined as the minimum ratio of the minimum closing force in the passive area over the maximum closing force of the active area in several veticals (see fig. 5b). The authors propose that, until more experience is gathered, the safety factor (n) should equal a minimum of 1.3. This is in accordance with the requirements for the conventional Bishop analysis used for embankments in the lower Meuse-Rhine delta.
In the Spencer analysis, a refinement can be made by iterating for the slope of the inter slice forces that yields the maximum inter slice force.

3.2.2 Deformations during uplift.

If above calculated factor of safety (n) is acceptable, loss of function of the embankment still may occur due to unacceptable compression of the marsh.
Under uplift conditions, the shear resistance in the sand/peat interface is reduced. This means a shift in boundary conditions. If the mobilization of the shear resistance in the active area is complete, uplift will have little or no direct effect on the inter slice forces in the embankment itself. However, under the berm and more beyond, horizontal pressures will increase, due to the loss of shear strength in the interface surface. With the determination of the water head as described, the shear resistance in the interface can be calculated and hence the increase of the interslice forces. Taking the stiffness of the berm and the peat under and beyond it into account, horizontal yielding and accumilated displacements can be approximated by taking this area as horizontal, compressible, partly floating beam (eq. 6)

$$\Delta L = \Sigma\{(1-\nu^2).L_i.\Delta F_{h,i}/(d.E_{u,i})\} \qquad \text{(eq. 6)}$$

in which: ΔL = total compression of the passive area
$\Delta F_{h,i}$ = increment of the hor. force in slice i.
L_i = length of slice i.
d = thickness of the aquitard.
$E_{u,i}$ = Young's modulus (undrained) for slice i.

The accuracy of the calculated compression of the marsh is especially dependent on the estimation of the increment of the horizontal force. For the determination of this increment it is important to take the previous stress history into account. Due to earlier uplift conditions and also due to the construction of the embankment, the marsh might have been exposed to high horizontal forces. During construction the active area under the embankment is exposed to high excess pore pressures, throughwhich less shear resistance can be mobilized and as a result the marsh is temporarily exposed to higher horizontal forces. Hence for a correct estimation of the compression of the marsh due to uplift during a design storm, a horizontal pre-consolidation force needs to be determined.

4 ACKNOWLEDGEMENTS

The authors express their special thanks to A.Verruyt and F.B.J.Barends, whose instructive recommendations have been highly appreciated.

5 LITERATURE.

- Baalen, M. van (1988): "Stabiliteit en deformatie bij opdrijven", Delft Geotechnics, SE 701210/3 (in Dutch).
- Barends, F.B.J. (1982): "Transient flow in leaky aguifers" Proc. of the Int. Conf. on Modern Approach to Groundwater Resources Management, Capri.
- Barends, F.B.J. (1988): "Opdrijven van 't achterland bij hoogwater", Delft Geotechnics, CO-290831/2.
- Bauduin, C.M. (1985): "Studie onderzoek naar de oorzaken van de afschuiving in Streefkerk". DG-rapport SE-690470 (in Dutch).
- Bauduin, C.M., Barends, F.B.J. (1988): Tidal Response under Dutch dikes, H2O (21),nr.1,pg 2-5 (in Dutch).
- Hird, C.C., Marsland, A., Schofield, A.N. (1978): "The development of centrifugal models to study the influence of uplift pressure on the stability of a flood bank". Geotechnique (28), no. 1, pp. 85 - 106.
- Marsland, A. Randolph, M.J. (1978): "A study of the variation and effects of water pressures in the pervious strata underlying Crayford Marshes". Geotechnique (28) no. 4, pp. 435 - 464.
- Marsland, A. (1961): "A study of a breach in an earthen embankment caused by uplift pressures". Proc. of the fifth ICMSFE , pp. 663 - 668.
- Padfield, C.J. Schofield, A.N. (1983): "The development of centrifugal models to study the influence of uplift pressures on the stability of a flood bank". Geotechnique (33), no. 1, pp. 56 - 66.
- Teunissen, J.A.M., Calle, E.O.F., Bauduin, C.M. (1986): "Analysis of failure of an embankment on soft soil, a case study". 2nd. Int. Conf. Num. Mod. in Geomechanics, Ghent, pp. 617 - 626.
- Vermeer,P.A., Ernst,R.J., van Dommelen,A.E. 1984: Stability computations using FEM analysis, Civiele & Bouwkundige Techniek - nr.10. (in Dutch)